ACTIVE MEDIA

PACS numbers: 42.55.Lt; 42.60.Lh
DOI: 10.1070/QE2007v037n02ABEH013166

Gain dynamics in a pulsed laser amplifier on CO – He, CO – N_2 and CO – O_2 gas mixtures

S.V. Vetoshkin, A.A. Ionin, Yu.M. Klimachev, A.Yu. Kozlov,
A.A. Kotkov, O.A. Rulev, L.V. Seleznev, D.V. Sinitsyn

***Abstract*. Small-signal gain (SSG) dynamics $G(t)$ in the active medium of a pulsed laser amplifier operating on the $v+1 \rightarrow vP(J)$ vibrational – rotational transitions of the CO molecule, including high ($v > 15$) vibrational transitions, is studied experimentally. It is demonstrated that as the vibrational number increases from 7 to 31, G changes with time slower, while G_{max} decreases in this case by three times. It is found that at a fixed value of v the rate of the SSG rise increases with increasing the rotational number $J > 6$. It is shown that in oxygen-containing gas mixtures ($CO:O_2 = 1:19$) the value of G_{max} at low vibrational levels (for $v < 13$) can substantially exceed G_{max} in mixtures containing nitrogen ($CO:N_2 = 1:19$) instead of oxygen. It is found that the efficiency (47 %) of a CO laser on mixtures with a high concentration of oxygen considerably exceeds the efficiency (30 %) of a CO laser operating on a nitrogen-containing mixture.**

Keywords: *vibrational exchange, carbon oxide, pulsed discharge, active medium, laser amplifier, CO laser.*

1. Introduction

A molecular CO laser can operate on vibrational – rotational transitions both in the $v+1 \rightarrow v$ fundamental vibrational transition band (at wavelengths 4.6 – 8.3 μm [1, 2]) and in the $v+2 \rightarrow v$ band of the first vibrational overtone (2.5 – 4.2 μm [3, 4]). It has been shown in [5] that in the active medium of a pulsed overtone-transition CO laser, the small-signal gain (SSG) G has the largest values in the wavelength range from 3 to 4 μm corresponding to the $v = 20 – 35$ vibrational transitions. Interest in the overtone CO laser is caused mainly by this spectral range. First, it overlaps the transparency window of atmosphere, which allows the transport of laser radiation in atmosphere with low losses [6], and, second, many molecules have absorption lines in this wavelength range, which often coincide with spectral lines of the overtone CO laser [7]. This feature can be used in different applications, for example, to monitor atmosphere. In this connection, the problem of expanding the radiation spectrum of a supersonic overtone CO laser to the wavelength range corresponding to high overtone transitions has been studied in [8]. Simulation of the active medium of such a laser on a pulsed laser setup has shown that the time of flight of excited gas from the pump region to the laser cavity was insufficient to achieve the threshold value of the SSG at high vibrational transitions.

The SSG dynamics $G(t)$ in the active medium of a CO laser is caused by the population of vibrational levels upon vibrational exchange between molecules, the noticeable role at high vibrational transitions ($v > 15$) being played by multiquantum and asymmetric exchange [5, 9]. In this case, the value of G at vibrational – rotational transitions changes with time almost similarly both for overtone and fundamental vibrational transitions [8, 10]. Therefore, the data on the temporal dynamics of the SSG at the fundamental vibrational transition band can be also used to develop overtone CO lasers. Earlier, the SSG dynamics was measured by the method of probing the active medium of a pulsed CO laser amplifier only for low ($v < 15$) transitions in the fundamental vibrational transition band [11, 12]. However, in the development of fast-flow CO lasers (see, for example, [8, 13 – 17]), which could operate both at low and high vibrational transitions, it is important to know how fast the value of G changes under different pump conditions. The aim of this paper is to study experimentally the effect of the specific energy input, density and composition of the CO – He, CO – N_2 and CO – O_2 gas mixture on the rate of change in the SSG in a wide range of vibrational transitions of the CO molecule, including high $v > 15$ transitions.

2. Experimental setup

A pulsed e-beam sustained discharge laser setup with active medium of length 1.2 m was used as a laser amplifier [18]. The working gas mixture was cooled through the side walls of the discharge chamber. In the active medium under study, the gas temperature T before the discharge pulse was $\sim 108 \pm 3$ K for the CO – He mixture and 117 ± 4 K for the CO – N_2 and CO – O_2 mixtures. The gas density N_g in the discharge chamber in different experiments varied from 0.04 to 0.12 amagat (1 amagat is the gas density under normal conditions). The pulsed pumping of the medium is characterised by the average specific energy input Q_{in}, which could be varied from 100 to 1000 J L^{-1} amagat $^{-1}$ (the difference in the values of the average and local energy inputs was discussed in [9]).

The SSG was measured by using a dc-discharge-pumped cw frequency-selective low-pressure CO laser with cryogen

S.V. Vetoshkin, A.A. Ionin, Yu.M. Klimachev, A.Yu. Kozlov, A.A. Kotkov, O.A. Rulev, L.V. Seleznev, D.V. Sinitsyn P.N. Lebedev Physics Institute, Russian Academy of Sciences, Leninsky prosp. 53, 119991 Moscow, Russia; e-mail: aion@sci.ebedev.ru

Received 28 March 2006; revision received 22 September 2006
Kvantovaya Elektronika **37** (2) 111 – 117 (2007)
Translated by I.A. Ulitkin

cooling of the active medium of length 1 m as a probe laser [18]. The probe CO laser operated in the fundamental vibrational transition band at more than 200 spectral lines (vibrational transitions from $v = 5$ to $v = 31$). The SSG in the discharge chamber was measured by positioning the probe laser beam of diameter 1 cm in the centre of the interelectrode gap of height 9 cm and width 16 cm. The output power of the laser radiation incident on and transmitted through the laser amplifier was measured with Hg–Cd–Zn–Te PEM-L-3 photodetectors. The intensity of the probe laser beam (no more than 1 W cm^{-2}) was much lower than the gain-saturation intensity ($\sim 10^2$ W cm^{-2} [19]) in the active medium of the pulsed laser amplifier. The output signals from photodetectors were recorded with C8-14 and Tetronix TDS1012 oscilloscopes. The dependence of $G(t)$ was calculated by analysing the detected signals, the absolute error in the values of G being 0.1 m^{-1}.

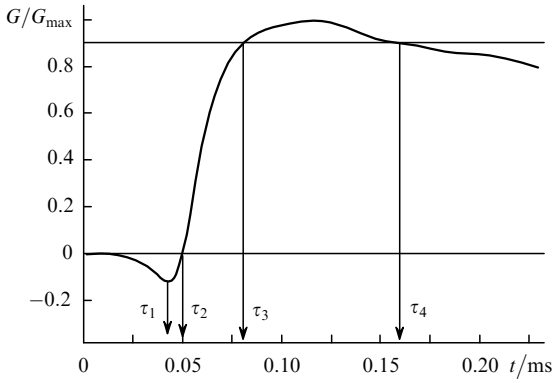

Figure 2. Determination of times $\tau_1 \div \tau_4$ by the example of the normalised value $G(t)/G_{max}$ for the $16 \rightarrow 15P(11)$ transition. Other conditions are as in Fig. 1.

3. Radiation amplification in the CO–He mixture

Figure 1 shows the temporal dynamics of the SSG in the CO : He = 1 : 4 mixture normalised to the maximum value of G_{max} for each of four vibrational–rotational transitions for $v = 15, 19, 26$ and 31. The instant of time equal to zero ($t = 0$) corresponds to the onset of the pump pulse of the active medium in the laser amplifier. The value of G changes with time as follows: radiation absorption ($G < 0$) takes place in the medium, which appears at the beginning of the population of vibrational levels, then, inverse population is formed at vibrational–rotational transitions and radiation amplification ($G > 0$) occurs, which rapidly increases till the maximum G_{max} and then slowly decreases. The lifetime of the inverse population, i.e. the time interval during which G is positive, can exceed the pump-pulse duration by many times. In the CO : He = 1 : 4 mixture ($N_g = 0.12$ amagat), the time interval, within wich $G(t) > 0.2G_{max}$, achieved 4 ms, i.e. exceeded the pump-pulse duration by two orders of magnitude. To study the change in the SSG dynamics as a function of excitation conditions of molecules, we determined four instants of time (Fig. 2), each of them corresponding to certain values of the SSG. For τ_1, radiation absorption achieves its maximum (in modulus) value, for τ_2 the absorption is replaced by the radiation amplification, $G(t = \tau_2) = 0$,

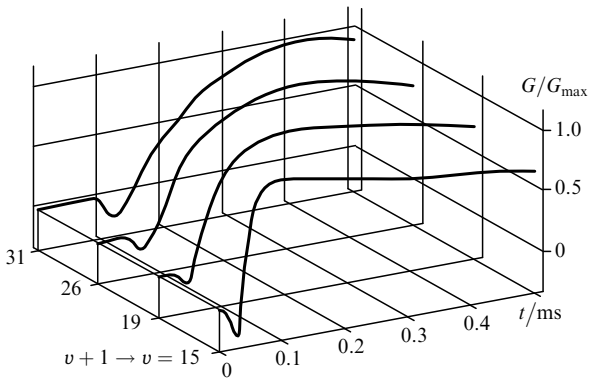

Figure 1. Small-signal gain $G(t)$ normalised to the maximum value of G_{max} for the $16 \rightarrow 15P(11)$, $20 \rightarrow 19P(14)$, $27 \rightarrow 26P(9)$, $32 \rightarrow 31P(9)$ transitions. The mixture is CO : He = 1 : 4, $N_g = 0.12$ amagat, $Q_{in} = 250$ J L^{-1} amagat^{-1}.

for τ_3 and τ_4 the radiation amplification achieves the level $G(t = \tau_3) = G(t = \tau_4 > \tau_3) = 0.9G_{max}$ at the leading and trailing edge of the gain pulse, respectively.

The difference τ_2 and τ_3 ($\tau_{32} = \tau_3 - \tau_2$) characterises the duration of the SSG rise in the leading edge of the gain pulse, while $\tau_{43} = \tau_4 - \tau_3$ characterises the duration of the top of the gain pulse. The relative error in the measurement of times $\tau_1 \div \tau_3$ was 4 %–8 % and τ_4 – 7 %–15 % [due to a slow decrease in $G(t)$ at the trailing edge of the gain pulse].

As the vibrational number v increases (all other conditions being the same), times $\tau_1 \div \tau_4$ also increase, because high vibrational levels are populated during the vibrational–vibrational exchange due to the vibrational energy concentrated at lower levels. In this case, the SSG grows slower, which is manifested in Fig. 1 as an increase in the time delay of the radiation amplification (times τ_1 and τ_2) and duration of the leading edge (τ_{32}). Figure 3 presents the dependences of $\tau_1 \div \tau_4$ on v for three values of the specific energy input Q_{in}. As the vibrational number v increased from 15 to 31, the values of $\tau_1 \div \tau_4$ increased by three–four times. The change in the dependence $\tau_4(v)$ with increasing the specific energy input Q_{in} is obviously caused by the heating of the gas mixture after the pump pulse. Values of the rotational numbers J for probe vibrational–rotational transitions are presented in Table 1.

An increase in the rotational number J within one vibrational transition leads to a decrease in $\tau_1 \div \tau_3$. Figure 4 presents the values of $\tau_1 \div \tau_3$ for eleven vibrational–rotational transitions belonging to one vibrational band ($10 \rightarrow 9$). The strongest relative change was observed for τ_2 and τ_3: the increase in J from 6 to 16 leads to a decrease in their values by half. Similarly, the duration of the leading edge of the SSG pulse τ_{32} decreased from 0.140 to 0.065 ms, and τ_1 decreased in this case by one and a half (from 0.048 to 0.032 ms). Due to the nonuniformity of the top of the gain pulse, the measurement error for time τ_4 was approximately 0.02 ms, hence, a small decrease in τ_4 (by 0.04 ms for $\langle \tau_4 \rangle = 0.45$ ms) with increasing J had a character of a tendency.

The observed changes in times $\tau_1 \div \tau_3$ as a function of the number J is caused by nonequilibrium vibrational exchange processes. It was shown in [18] that the inequality $d\tau_2/dJ < 0$ is fulfilled if the population of the upper vibrational level N_{v+1} increases faster than that of the lower level N_v,

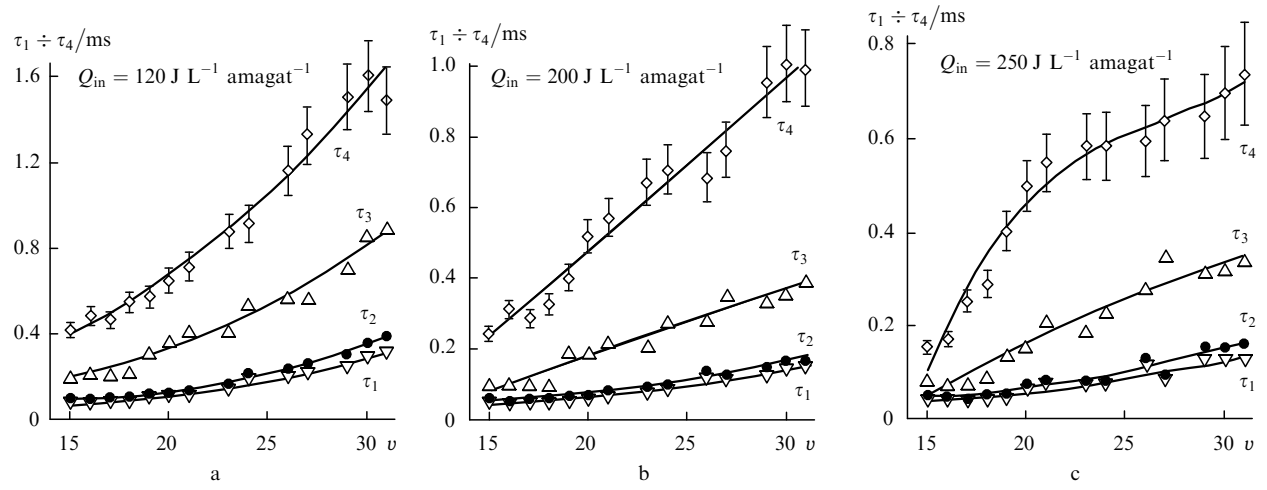

Figure 3. Dependences of times $\tau_1 \div \tau_4$ on the vibrational number v for different values of the specific energy input Q_{in} for the CO : He = 1 : 4 mixture; $N_g = 0.12$ amagat. The values of the rotational numbers J are presented in Table 1.

Table 1. Rotational numbers J for the probed $v+1 \rightarrow v$ P(J) vibrational–rotational transitions (Fig. 3).

v	15	16	17	18	19	20	21	23	24	26	27	29	30	31
J	11	10	11	12	14	14	14	11	13	9	13	8	8	9

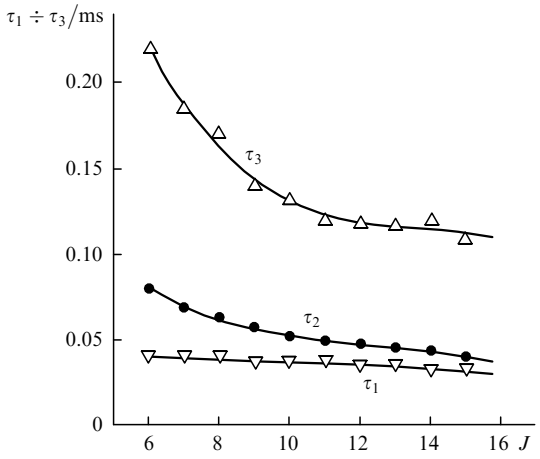

Figure 4. Dependences of times $\tau_1 \div \tau_3$ at the $10 \rightarrow 9$P(J) transition on the rotational number J for the CO : He = 1 : 4 mixture for $N_g = 0.12$ amagat, $Q_{in} = 100$ J L^{-1} amagat^{-1}.

$$\dot{N}_{v+1} > \dot{N}_v \equiv \frac{dN_v}{dt}, \tag{1}$$

and this occurs during the formation of a nonstationary vibrational distribution function in the form of a plateau. In this case, the change in the gas temperature was assumed small and weak dependences of the rotational constant B_v, the emission wavelength and the linewidth on J were neglected [18, 20]. We will show that the more general statement for the same assumptions is valid: if condition (1) is fulfilled, the rate of the SSG rise increases with increasing J. Let us introduce the notation $X = J/J_0$, where $J_0 = J_B + 0.5 = [kT/(2B_v)]^{0.5}$; J_B corresponds to the maximum of the Boltzmann distribution of the population of the vibrational level v over the rotational sublevels J; k is the Boltzmann constant; and T is the gas temperature. For the $v+1 \rightarrow v$P(J) transition, the rate of change in the SSG is

$$\dot{G} \sim X \exp(-0.5X^2)\left[\dot{N}_{v+1} \exp\left(\frac{0.5X}{J_0}\right) - \dot{N}_v \exp\left(-\frac{0.5X}{J_0}\right)\right]. \tag{2}$$

If relation (1) is fulfilled, the SSG increases ($\dot{G} > 0$). By differentiating expression (2) over the variable X, we arrive to the relation

$$\frac{d\dot{G}}{dX} > 0,$$

if

$$\frac{\dot{N}_{v+1}}{\dot{N}_v} > \frac{1 - X^2 - 0.5X/J_0}{1 - X^2 + 0.5X/J_0} \exp\left(-\frac{X}{J_0}\right) \equiv f(X). \tag{3}$$

For $X > 1.5$ and $J_0 > 1$ ($J_0 = 4.6$ in the experiment), the function $f(X)$ takes the values smaller than unity. Therefore, if condition (1) is fulfilled, i.e. during the formation of the plateau of the vibrational distribution function, relations (3) are valid for $J > 1.5J_0$ and the SSG increases faster with increasing J (see Fig. 4 for $J > 6$).

An increase in the specific energy input Q_{in} from 120 to 250 J L^{-1} amagat^{-1} leads to a decrease in $\tau_1 \div \tau_4$ (Fig. 3) and an increase in G_{max}. The maximum value of G_{max} was achieved at low vibrational transitions and was 3.3 m^{-1} for the $8 \rightarrow 7$P(10) transition. For high transitions, the values of G_{max} were also rather large: for example, for the $31 \rightarrow 30$P(8) transition, $G_{max} = 1.2$ m^{-1}. For the specific energy input $Q_{in} = 250$ J L^{-1} amagat^{-1}, the values of G_{max} for all transitions were on average by 1.2 times greater than for $Q_{in} = 200$ J L^{-1} amagat^{-1} and by 2.6 times greater than for $Q_{in} = 120$ J L^{-1} amagat^{-1}.

An increase in the gas mixture density N_g leads to the increase in the collision frequency and rates of kinetic processes of the energy exchange between molecules. Therefore, the values of $\tau_1 \div \tau_4$, which characterise the rate of the SSG change, should decrease in this case. Their change as a function of the gas mixture density is presented in Table 2 by the example of the $19 \rightarrow 18$P(11) transition for two specific energy inputs. Indeed, the values of $\tau_1 \div \tau_4$

Table 2. Times $\tau_1 \div \tau_4$ at the $19 \rightarrow 18P(11)$ transition for three values of the gas density N_g and two values of the specific energy input Q_{in} in the $CO:He = 1:4$ mixture.

Q_{in}/ J L^{-1} amagat^{-1}	N_g/amagat	G_{max}/m^{-1}	τ_1/ms	$\tau_1 N_g$/μs amagat	τ_2/ms	$\tau_2 N_g$/μs amagat	τ_3/ms	$\tau_3 N_g$/μs amagat	τ_4/ms	$\tau_4 N_g$/μs amagat
	0.04	1.0	0.090	3.6	0.120	4.8	0.26	10.4	0.70	28
250	0.06	1.4	0.070	4.2	0.090	5.4	1.190	11.4	0.56	34
	0.12	1.5	0.040	4.8	0.050	6.0	0.090	10.8	0.29	35
Average value $\langle \tau_n N_g \rangle$/μs amagat				4.2 ± 0.3		5.4 ± 0.3		10.9 ± 0.3		32 ± 2
	0.04	0.5	0.22	8.8	0.29	11.6	0.82	33	2.30	92
150	0.06	0.7	0.140	8.4	0.180	10.8	0.43	26	1.45	87
	0.12	0.8	0.080	9.6	0.100	12.0	0.22	26	0.60	72
Average value $\langle \tau_n N_g \rangle$/μs amagat				8.9 ± 0.4		11.5 ± 0.4		28 ± 2		84 ± 6

decreased with increasing the density N_g; the product $\tau_n N_g$ ($n = 1 - 4$) being slightly different from the average value, i.e. times changed inversely proportional to the gas density, $\tau_n \sim N_g^{-1}$. Note that for $N_g = 0.04 - 0.06$ amagat and $Q_{in} = 150$ J L^{-1} amagat^{-1}, the duration of the gain-pulse top τ_{43} exceeded 1 ms due to the low rate of relaxation processes. The increase in the gas density and the energy input allows one to reduce the time of the SSG rise (τ_{32}) and increase G_{max}. For example, for the $19 \rightarrow 18P(11)$ transition the time interval τ_{32} decreased more than an order of magnitude – from $\tau_{32} = 0.53$ ms for $N_g = 0.04$ amagat and $Q_{in} = 150$ J L^{-1} amagat^{-1} to $\tau_{32} = 0.040$ ms for $N_g = 0.12$ amagat and $Q_{in} = 250$ J L^{-1} amagat^{-1}, while G_{max} increased in this case by three times (from 0.5 to 1.5 m^{-1}).

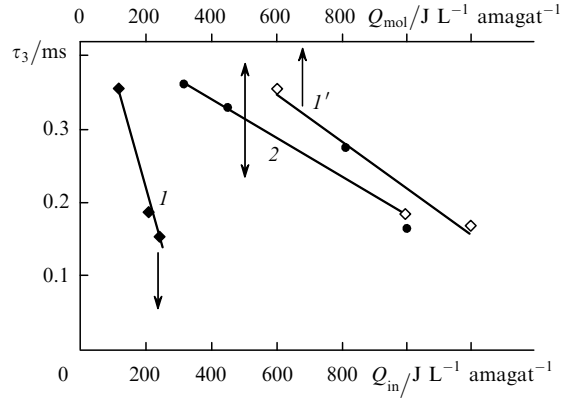

Figure 5. Dependences of τ_3 [the $21 \rightarrow 20P(J)$ transition] on the specific energy input Q_{in} for for $N_g = 0.12$ amagat for the mixtures $CO:He = 1:4$, $J = 14$ (*1*, ◆) (*1′*, ◇ recalculated for $Q_{mol} = 5Q_{in}$) and $CO:N_2 = 1:9$, $J = 11$ (*2*, ●).

4. Radiation amplification in the CO – N_2 gas mixture

The presence of other molecular gases in the gas mixture with CO leads to redistribution of the vibrational energy between molecules and affects the dependence $G(t)$. In Table 3, times $\tau_1 \div \tau_4$ are compared by the example of the $21 \rightarrow 20P(11)$ vibrational – rotational transition in $CO:N_2 = 1:9$ and $CO:He = 1:4$ mixtures for the same gas density $N_g = 0.12$ amagat. For close values of the specific energy input ($Q_{in} = 250 - 300$ J L^{-1} amagat^{-1}), the values of $\tau_1 \div \tau_4$ in the nitrogen-containing mixture were significantly higher than in the helium-containing mixture. An increase in the energy input for the nitrogen mixture resulted in a decrease of times $\tau_1 \div \tau_4$ (Fig. 5 shows a change in τ_3). In the nitrogen mixture for $Q_{in} = 800$ J L^{-1} amagat^{-1}, τ_1 and τ_2 were smaller than in the helium mixture for $Q_{in} = 250$ J L^{-1} amagat^{-1}, but the value of τ_3 in the CO – N_2 mixture (0.27 ms) was higher than in the CO – He mixture (0.155 ms). Note that under the same pump conditions, analogous relation between the times $\tau_1 \div \tau_3$ at low vibrational transitions was observed.

For the $8 \rightarrow 7P(10)$ transition, the values of τ_1 and τ_2 in the nitrogen mixture were lower, while the time $\tau_3 = 0.055$ ms was greater than in the helium mixture ($\tau_3 = 0.045$ ms). In this case, G_{max} at the $8 \rightarrow 7P(10)$ transition for both mixtures were nearly the same ($G_{max} = 3.3 \pm 0.1$ m^{-1}) despite the difference in Q_{in}. A larger fraction of energy (70 % – 90 %) supplied in the gas mixture upon pulse pumping is stored in the form of vibrational energy of molecules (see, for example, [21], Chapter 10, Section 4). If we recalculate the specific energy input by the content of molecules in the gas mixture (Q_{mol}), the energy input only for active molecules in the $CO:He = 1:4$ mixture should be increased by five times ($Q_{mol} = 5Q_{in}$); for the nitrogen mixture, $Q_{mol} = Q_{in}$. Therefore, while comparing the radiation amplification in gas mixtures containing atomic and molecular gases, one should apparently compare the values of Q_{mol}. In particular, two dependences of τ_3 on the energy input Q_{in} presented in Fig. 5 for two mixtures [(*1*) and (*2*)], which are recalculated by the value of Q_{mol} prove to be very close [(*1′*) and (*2*)].

Both in the $CO:N_2 = 1:9$ and $CO:He = 1:4$ mixtures for $v > 7$, the increase in the vibrational number v (other conditions being the same) leads to a decrease in G_{max} (Fig. 6) and a slower change in the gain (times $\tau_1 \div \tau_4$ increased). A rather slow change in $G(t)$ was observed in the nitrogen mixture at a low gas density and a high concentration of nitrogen. Figure 7a presents the temporal SSG dynamics at four vibrational transitions ($v = 12$, 14, 15 and 17) for the $CO:N_2 = 1:19$ mixture at $N_g =$

Table 3. Values of $\tau_1 \div \tau_4$ at the $21 \rightarrow 20P(J)$ transition for two gas mixtures for the gas density $N_g = 0.12$ amagat.

Mixture	Q_{in}/J L^{-1} amagat^{-1}	Q_{mol}/J L^{-1} amagat^{-1}	τ_1/ms	τ_2/ms	τ_3/ms	τ_4/ms
CO – N_2 ($J = 11$)	300	300	0.085	0.125	0.36	0.81
	800	800	0.055	0.072	0.27	0.55
CO – He ($J = 14$)	250	1250	0.072	0.077	0.155	0.53

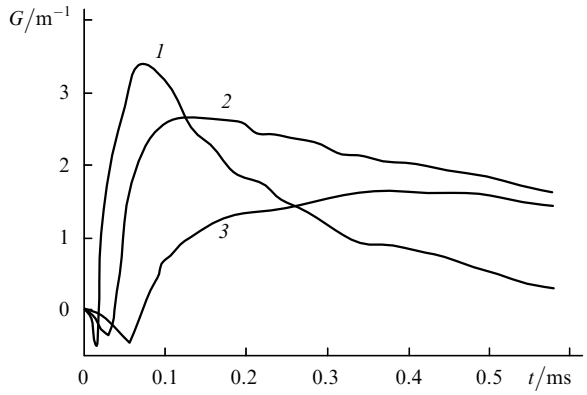

Figure 6. Values of $G(t)$ in the $CO:N_2 = 1:9$ mixture at $8 \rightarrow 7P(10)$ (*1*), $14 \rightarrow 13P(10)$ (*2*) and $21 \rightarrow 20P(11)$ (*3*) transitions for $N_g = 0.12$ amagat, $Q_{in} = 800$ J L^{-1} amagat^{-1}.

0.04 amagat, τ_3 exceeding 1 ms for $v = 12$ and increasing to 1.7 ms for $v = 17$.

5. Radiation amplification in the CO – O_2 gas mixture

It was shown in [22, 23] that a small addition of CO molecules (1 % – 10 % from the concentration of oxygen) in the oxygen rich gas mixture allows the increase in the energy supplied in this gas mixture upon pulsed electroionisation discharge. We performed laser probing of the oxygen rich gas mixture ($CO:O_2 = 1:19$) at transitions of the CO molecule. The dynamics of $G(t)$ at high vibrational transitions in the $CO:O_2 = 1:19$ mixture (Fig. 7b) significantly differed from the dynamics of $G(t)$ in the $CO:N_2 = 1:19$ mixture (Fig. 7a). For $v = 12$, the values of $\tau_1 \div \tau_4$ in the CO – O_2 mixture were smaller than in the CO – N_2 mixture while the value of G_{max}, vice versa, was twice larger. For $v = 14$ in the oxygen mixture, the values of the SSG appeared during short time while for higher values of the vibrational number ($v > 14$), the radiation amplification, unlike the nitrogen mixture, did not increase ($G \leqslant 0$).

Radiation absorption at high vibrational transitions of the CO molecule is related to the intermolecular vibrational exchange:

$$CO(v) + O_2(0) \leftrightarrow CO(v-1) + O_2(1) + \Delta E_{vJ}, \qquad (4)$$

where ΔE_{vJ} is the difference in energies of the vibrational – rotational transitions of molecules involved in the exchange. The rate of exchange (4) increases with increasing the vibrational number v because the energy of vibrational – rotational transitions of the CO molecule for $v \sim 20$ approaches the excitation energy of the O_2 molecules in the $0 \rightarrow 1$ ($\Delta E_{vJ} \approx 0$) vibrational transition band. Effect of exchange process (4) on the stationary vibrational distribution function of the CO molecules was discussed earlier, for example, in [24]. In the processes of intermolecular exchange (4) there occurs dissipation of the vibrational energy of those CO molecules for which $\Delta E_{vJ} \sim kT$, and, hence, when the

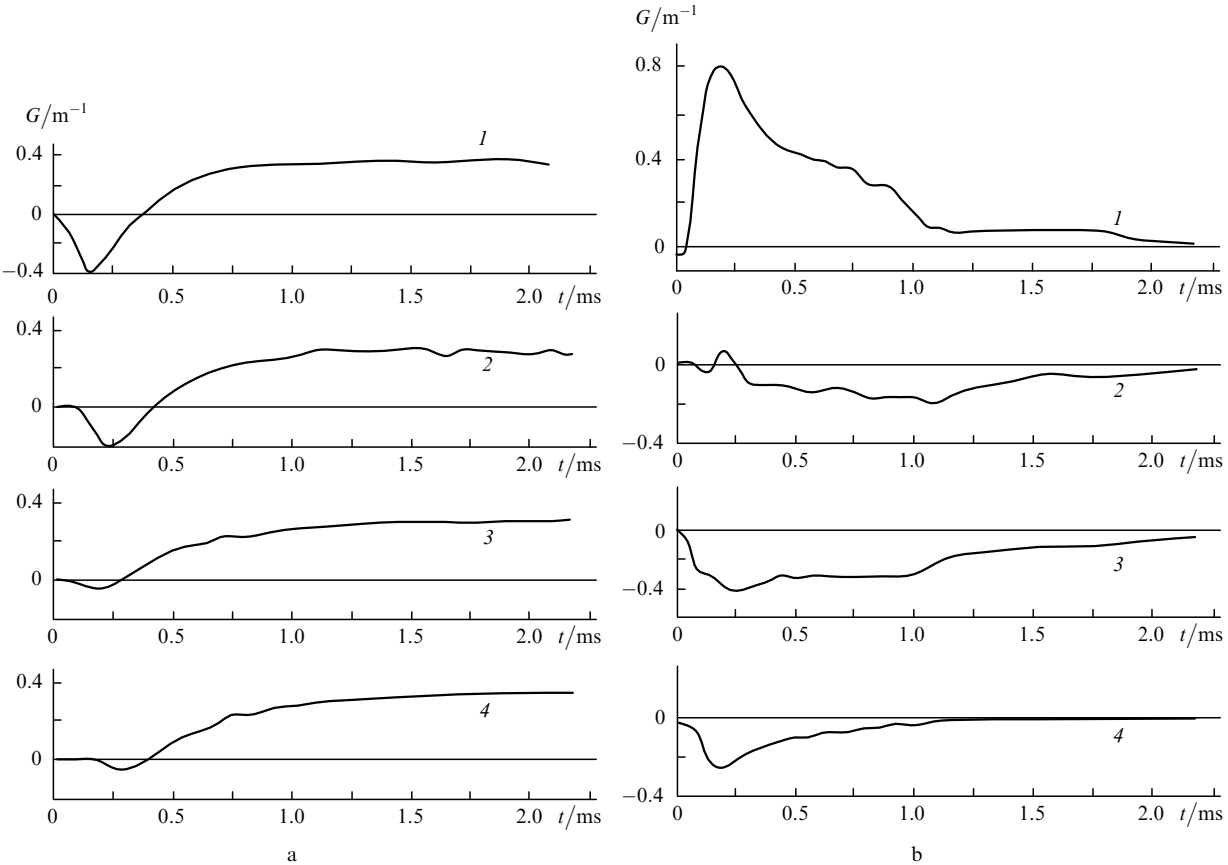

Figure 7. Values of $G(t)$ in the $CO:N_2 = 1:9$ (a) and $CO:O_2 = 1:19$ (b) mixtures at $13 \rightarrow 12P(13)$ (*1*), $15 \rightarrow 14P(14)$ (*2*), $16 \rightarrow 15P(13)$ (*3*) and $18 \rightarrow 17P(12)$ (*4*) transitions for $Q_{in} = 190$ J L^{-1} amagat^{-1}, $N_g = 0.04$ amagat.

vibrational number v increased higher of some value depending on the gas temperature, the SSG value decreases (for $v > 13$ under our experimental conditions). At the same time, the maximum value of the gain G_{max} at the $13 \rightarrow 12P(13)$ transition in the $CO:O_2 = 1:19$ mixture was significantly higher than in the $CO:N_2 = 1:19$ mixture (Fig. 7). During exchange (4), CO molecules undergo the $v \rightarrow v-1$ transition downward to one vibrational level, which, obviously, favours the amplification of radiation at vibrational–rotational transitions located lower than those that are efficiently involved in the intermolecular exchange.

Earlier [5] in the CO–He–N_2 mixture an analogous effect of the intermolecular asymmetric exchange

$$CO(v) + N_2(0) \leftrightarrow CO(v-2) + N_2(1) + \Delta E_{vJ} \qquad (5)$$

by the value G_{max} was observed in the active medium of the pulsed overtone CO laser at $v = 34-36$ transitions. As the concentration of nitrogen molecules was increased, the efficient depopulation of vibrational levels $v > 37$ led to a decrease in G_{max} at $38 \rightarrow 36$ transitions, and, vice versa, to an increase in G_{max} at $36 \rightarrow 34$ transitions. Therefore, the performed experiments have demonstrated that in the oxygen rich gas mixtures ($CO:O_2 = 1:19$) the value of G_{max} at vibrational transitions for $v < 13$ can be twice that in the mixture with nitrogen ($CO:N_2 = 1:19$) instead of oxygen, which is, apparently, caused by intermolecular vibrational exchange (4) between CO and O_2 molecules.

The possibility of lasing at CO transitions in the oxygen rich gas mixture was demonstrated in [22]. By continuing the experiment, we have found that the efficiency η of this laser can exceed the efficiency of the CO laser with the nitrogen-containing gas mixture. The laser cavity consisted of two mirrors: a highly reflecting copper mirror with the radius of curvature 10 m and a plane semitransparent mirror with the transmission coefficient 50 %. The emission spectrum of the laser with the oxygen-containing gas mixture $CO:O_2:Ar = 1:10:10$ was in the wavelength range from 4.95 to 5.42 μm and consisted of ~30 lines corresponding to the $v = 3-10$ vibrational–rotational transitions of the CO molecules. Figure 8a presents the dependence of the specific lasing energy extraction Q_{las} on the specific energy input Q_{in} for two gas mixtures: $CO:O_2:Ar = 1:10:10$ and $CO:N_2:Ar = 1:10:10$. The lasing energy extraction in the oxygen-containing mixture for $Q_{in} = 170$ J L^{-1} amagat^{-1} was two times higher than in the nitrogen-containing mixture.

The energy conversion efficiency of the pump to laser radiation characterises the ratio between the local values of the energy extraction and input. However, the measurement of the local value of the specific energy input Q_{loc} in the pulsed discharge plasma is a difficult experimental problem. In [9], the calculated and experimental data on the temporal SSG dynamics (experiments described in the present paper and in [9] were performed on the same laser setup) were compared to show that the ratio between the local and average values of the specific energy input Q_{loc}/Q_{in} can vary from 0.63 to 0.72 depending on the excitation conditions. The lasing efficiency ($\eta = Q_{las}/Q_{loc} \times 100\,\%$) in the CO–$O_2$–Ar mixture achieved 47 % (Fig. 8b), i.e. exceeded by 1.6 times the efficiency η of the CO laser in the CO–N_2–Ar mixture (30 %), the ratio between the efficiencies achieving 2.5 for $Q_{in} = 100$ J L^{-1} amagat^{-1}. A decrease in the efficiency of the CO laser operating on the CO–O_2–Ar mixture for $Q_{in} > 170$ J L^{-1} amagat^{-1} can be explained by the gas heating [25] and the excitation of electronic states of molecular oxygen [22].

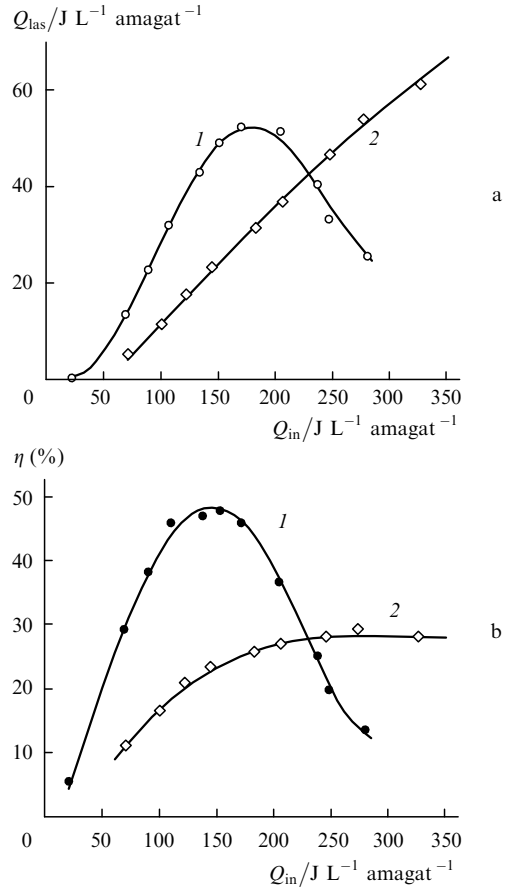

Figure 8. Dependences of the laser specific energy extraction Q_{las} (a) and the efficiency (b) on the average value of the specific energy input Q_{in} in $CO:O_2:Ar = 1:10:10$ (*1*) and $CO:N_2:Ar = 1:10:10$ (*2*) mixtures for $N_g = 0.08$ amagat.

6. Conclusions

The results of our experiments have demonstrated how the SSG dynamics changes at different vibrational–rotational levels of the CO molecule in the active medium of a pulsed laser amplifier as a function of the specific energy input, the gas density and the composition of the gas mixture (CO–He, CO–N_2, CO–O_2). It has been shown that the value of the SSG changes with time slower when the vibrational number v is increased from 7 to 31. It has been found that for a fixed value of v, an increase in the rotational number J leads to the increase in the rate of the SSG rise. It has been shown that the rate of the SSG change significantly increases with increasing the specific energy input. The highest measured gain (3.3 m^{-1} at the low $8 \rightarrow 7$ vibrational transition) was the same for $CO:He = 1:4$ and $CO:N_2 = 1:9$ mixtures and exceeded only by three times the maximum gain at the high $31 \rightarrow 30$ vibrational transition. We have demonstrated that depending on the gas mixture density, the parameters charachterising the temporal SSG dynamics change inversely proportional to the gas density. The obtained results can be used to develop an overtone fast-flow CO laser operating on high vibrational transitions.

It has been shown that in the oxygen containing gas mixtures ($CO:O_2 = 1:19$), the maximum value of the SSG

at low vibrational transitions can be twice as large as that in the mixtures in which nitrogen is used instead of oxygen ($CO:N_2 = 1:19$). It has been found that the efficiency of the CO laser on oxygen rich gas mixtures ($CO:O_2:Ar = 1:10:10$) can substantially exceed (for $Q_{in} = 100$ J L^{-1} amagat^{-1} – by 2.5 times) the efficiency of the CO laser on the nitrogen-containing mixture ($CO:N_2:Ar = 1:10:10$). In this case the maximum efficiency of the CO laser on the $CO:O_2:Ar = 1:10:10$ mixture achieved 47 %, which is considerably higher than the maximum efficiency of the CO laser (30 %) on the $CO:N_2:Ar = 1:10:10$ mixture.

Acknowledgements. This work was supported by the Russian Foundation for Basic Research (Grant No. 05-02-17656), AFRL, EOARD, International Scientific and Technical Centre (Project No. 2415-P) and the Program of Support of the Youth of the Educational and Scientific Centre of P.N. Lebedev Physics Institute.

References

1. Yardley J.T. *J. Molec. Spectr.*, **35**, 314 (1970).
2. McCord J.E., Ionin A.A., Phipps S.P., et al. *IEEE J. Quantum Electron.*, **36**, 1041 (2000).
3. Basov N.G., Ionin A.A., Kotkov A.A., et al. *Kvantovaya Elektron.*, **30**, 771 (2000) [*Quantum Electron.*, **30**, 771 (2000)].
4. Basov N.G., Ionin A.A., Kotkov A.A., et al. *Kvantovaya Elektron.*, **30**, 859 (2000) [*Quantum Electron.*, **30**, 859 (2000)].
5. Basov N.G., Ionin A.A., Klimachev Yu.M., et al. *Kvantovaya Elektron.*, **32**, 404 (2002) [*Quantum Electron.*, **32**, 404 (2002)].
6. Buzykin O.G., Ivanov S.V., Ionin A.A., et al. *Opt. Atmos. Okean.*, **14**, 400 (2001) [*Atmos. Ocean. Opt.*, **14**, 361 (2001)].
7. Buzykin O.G., Ivanov S.V., Ionin A.A., et al. *Izv. Ross. Akad. Nauk. Ser. Fiz.*, **66**, 962 (2002) [*Bulletin of the Russian Academy of Sciences*, **66**, 1055 (2002)].
8. Bohn W., von Bülow H., Dass S., et al. *Kvantovaya Elektron.*, **35**, 1126 (2005) [*Quantum Electron.*, **35**, 1126 (2005)].
9. Vetoshkin S.V., Ionin A.A., Klimachev Yu.M., et al. *Kvantovaya Elektron.*, **35**, 1107 (2005) [*Quantum Electron.*, **35**, 1107 (2005)].
10. Cacciatore M., Kurnosov A., Napartovich A., Shnyrev S. *J. Phys. B: Atomic, Molecular and Optical Physics*, **37**, 3379 (2004).
11. Boness M.J.W., Center R.E. *Appl. Phys. Lett.*, **26**, 511 (1975).
12. Basov N.G., Kazakevich V.S., Kovsh I.B., Mikryukov A.N. *Kvantovaya Elektron.*, **10**, 1049 (1983) [*Sov. J. Quantum Electron.*, **13**, 667 (1983)].
13. Bergman R.C., Rich J.W. *Appl. Phys. Lett.*, **31**, 597 (1977).
14. Klosterman E.L., Byron S.R. *J. Appl. Phys.*, **50**, 5168 (1979).
15. Gorshkov I.I., Ionin A.A., Kotkov A.A., et al. *Kratk. Soobshch. Fiz. FIAN*, (5), 31 (1989) [*Bulletin of the Lebedev Physics Institute*, (5), 40 (1989)].
16. Dymshits B.M., Ivanov G.V., Mescherskiy A.N., Kovsh I.B., *Proc. SPIE Int. Soc. Opt. Eng.*, **2206**, 109 (1994).
17. Golovin A.S., Gurashvili V.A., Kochetov I.V., et al. *Kvantovaya Elektron.*, **23**, 405 (1996) [*Quantum Electron.*, **26**, 395 (1996)].
18. Vetoshkin S.V., Ionin A.A., Klimachev Yu.M., et al. Preprint FIAN No. 13 (Moscow, 2005); Vetoshkin S.V., Ionin A.A., Klimachev Yu.M., et al. *J. Rus. Laser Research*, **27**, 33 (2006).
19. Elkin N.N., Kochetov I.V., Kurnosov A.K., Napartovich A.P. *Kvantovaya Elektron.*, **17**, 313 (1990) [*Sov. J. Quantum Electron.*, **20**, 252 (1990)].
20. Patel C.K.N. *Phys. Rev.*, **141**, 71 (1966).
21. Gorgiets B.F., Osipov A.I., Shelepin L.A. *Kinetic Processes in Gases and Molecular Lasers* (Amsterdam: Gordon and Breach Science Publishers, 1988; Moscow: Nauka, 1980).
22. Vagin N.P., Ionin A.A., Klimachev Yu.M., et al. *Kvantovaya Elektron.*, **34**, 865 (2004) [*Quantum Electron.*, **34**, 865 (2004)].
23. Ionin A.A., Klimachev Yu.M., Kotkov A.A., et al. RF Patent No. 2206495 (priority date 10.04.2002).
24. Plönjes E., Palm P., Lee W., et al. *Chem. Phys.*, **260**, 353 (2000).
25. Ionin A.A., Klimachev Yu.M., Kozlov A.Yu., et al. *Kvantovaya Elektron.*, **37**, 231 (2007) [*Quantum Electron.*, **37**, 231 (2007)].